Noname manuscript No.
(will be inserted by the editor)

NONLINEAR STABILITY AND TIME STEP SELECTION FOR THE MPM METHOD

Martin Berzins[1]

Received: date / Accepted: date

Abstract The Material Point Method (MPM) has been developed from the Particle in Cell (PIC) method over the last 25 years and has proved its worth in solving many challenging problems involving large deformations. Nevertheless there are many open questions regarding the theoretical properties of MPM. For example in while Fourier methods, as applied to PIC may provide useful insight, the non-linear nature of MPM makes it necessary to use a full non-linear stability analysis to determine a stable time step for MPM. In order to begin to address this the stability analysis of Spigler and Vianello is adapted to MPM and used to derive a stable time step bound for a model problem. This bound is contrasted against traditional Speed of sound and CFL bounds and shown to be a realistic stability bound for a model problem.

Keywords MPM Non-linear Stability

1 Introduction

The Material Point Method (MPM) may be viewed as being a solid mechanics method that is derived [26,27] from the fluid implicit particle, FLIP and PIC methods and which has had considerable success on large deformation problems. Despite this success many theoretical issues to do with MPM remain unresolved. One such issue is the stability of the method, given its non-linear nature. One approach is to use a Fourier-based analysis e.g. [7,19] or another is to use an energy-conservation analysis 'approach e.g. [1] is taken. However Wallstedt and Guilkey [29] rightly point out that the non-linear nature of the MPM scheme makes classic linear stability analysis inappropriate. Typically, approaches such as a speed of sound approach are used to define a time step, [12]. An alternative approach to stability s to consider conservation of energy. While energy conservation is of great importance it does not necessarily imply stability [20].

[1] SCI Institute, University of Utah, Salt Lake City, USA
mb@sci.utah.edu www.sci.utah.edu

The situation is similar for other particle methods. There is also much related work on SPH [14,18] and finite element methods, see [3–5] for a summary of this work. Belytschko and Xaio [5] address two sources of instability of their particle methods. The first one is a rank deficiency of the discrete equations that is similar to the ringing instability or the null space problem considered here and the second is a distortion of the material instability. The work on these methods deals with continually moving points without having a background grid as is used in MPM. For this reason it is not at all clear how the body of work introduced above immediately relates to MPM with its mixture of Lagrangian particles and a Eulerian background grid.

One way to start to address the issue of stability is is to note that the standard time integration methods used in MPM corresponds to the use of the semi-implicit Euler method, or symplectic Euler-A [16]. There is convergence and stability analysis of this method in [23] and this analysis is sufficiently general to be applied to the MPM, providing that care is taken with the non-linear nature of MPM. The intention here is to use this approach to shed some light on the non-linear stability of MPM by considering a one dimensional model problem as an ordinary differential equations system in the values at particles and nodes. While this does not address the well-known issues to do with ringing that has been previously considered [11,7], the aim is to consider how to bound the time step when non-linearity is taken into account. Consequently Section 2 described the MPM method and the model problem used, while Section 3 provides the theoretical framework for the stability analysis in Section 4 which leads to a stability result for the update strain last case. Numerical experiments as on a model problem used by [11] are reported in Section 5, show that the derived stability limit is of value for the model problem considered. This paper build on the conference paper [6] by extending the approach to the GIMP method and the update stress last approach together with computational results. In deriving the results here we will derive a stability condition that relates to the speed of sound condition used by [12].

2 A Simplified Form of MPM Method for Analysis

The description of MPM used here follows [11] in that the model problem used here is a pair of equations connecting velocity v, displacement u and density ρ (here assumed constant):

$$\frac{Du}{Dt} = v, \tag{1}$$

$$\rho \frac{Dv}{Dt} = \frac{\partial \sigma}{\partial x} + b, \tag{2}$$

with a linear stress model $\sigma = E\frac{\partial u}{\partial x}$ for which Young's modulus, E, is constant, a body force b and with appropriate boundary and initial conditions. For convenience a mesh of equally spaced $N+1$ fixed nodes X_i with intervals $I_i = [X_i, X_{i+1}]$, on on the interval $[a,b]$ is used where

$$a = X_0 < X_1 < ... < X_N = b, \tag{3}$$

$$h = X_i - X_{i-1}. \tag{4}$$

Further it is assumed that there are m particles between each pair of nodes, situated at x_p^n points where at each time step, $t^n = \delta t * n$, where n is the nth time step, and the computed solution at the pth particles will be written as $u_p^n = u(x_p^n, t^n)$. Suppose that the particles in interval i lie between X_i and X_{i+1} and have positions $x_{im+j}, j = 1, .., m$. The calculation of the internal forces in MPM at the nodes requires the calculation of the volume integral of the divergence of the stress, [29], which is written as

$$f_i^{int} = -\frac{1}{h}\sum_p D_{ip}^* \sigma_p V_p. \tag{5}$$

The coefficients D_{ip}^* may also be chosen to reproduce derivatives of constant and linear functions exactly, [11], in a similar way to that used in other particle methods e.g. [8]. The assumption here is that GIMP is being used [2]. A further simplification is to assume uniform particle masses and that the initial volume of the particles is uniform for the m particles in an interval. The particle volumes are defined using the absolute value of the deformation gradient, $|F_p^n|$, and the initial particle volume,

$$V_p^n = |F_p^n|\frac{h}{m}, \; where \; F_p^0 = 1. \tag{6}$$

From (5) the acceleration equation in MPM method after cancelling h and using constant density is:

$$\begin{aligned} a_i^{n+1} = & \frac{-1}{m}\Big(\sum_{x_p \in I_{i-2}} D_{ip}^{n*} \sigma_p^n |F_p^n| + \sum_{x_p \in I_{i-1}} D_{ip}^{n*} \sigma_p^n |F_p^n| + \\ & \sum_{x_p \in I_i} D_{ip}^{n*} \sigma_p^n |F_p^n| + \sum_{x_p \in I_{i+1}} D_{ip}^{n*} \sigma_p^n |F_p^n| \Big). \end{aligned} \tag{7}$$

The two terms involving particles $X_p \in I_{i-1}$ and $x_p \in I_{i+2}$ arise as GIMP is being used. The equation to update velocity at the nodes, as denoted by v_i^n is then given by

$$v_i^{n+1} = v_i^n + dt a_i^{n+1}. \tag{8}$$

Using linear interpolation gives the equation for the update of the particle velocity:

$$v_p^{n+1} = v_p^n + dt[\lambda_{i-1,p} a_{i-1}^{n+1} + \lambda_{i,p} a_i^{n+1} + \lambda_{i+1,p} a_{i+1}^{n+1} + \lambda_{i+2,p} a_{i+2}^{n+1}], x_p \in I_i \tag{9}$$

where λ_{ip} is defined by [2,24] . The use of GIMP basis functions would give rise to an extended stencil involving a_{i-1}^{n+1} and The equation for the particle position update is

$$x_p^{n+1} = x_p^n + v_p^{n+1} dt. \tag{10}$$

The immediate use of the updated velocity v_p^{n+1} in this and subsequent equations is the symplectic Euler method. The update of the deformation gradients and stresses is given using their linear spatial derivative defined by : which in the case of GIMP the derivative is represented by a four point stencil.

$$\frac{\partial v^{n+1}}{\partial x}(x_p) = \frac{1}{h}\sum_{j=i-1}^{i+2} \gamma_{j,p} v_j^{n+1}, x_p \in I_i. \; where \; -1 \le \gamma_{j,i} \le 1. \tag{11}$$

The following inequality will be useful later

$$\left| \frac{\partial v^{n+1}}{\partial x}(x_p) \right| \leq \frac{1}{h} \sum_{j=i-1}^{i+2} |v_j^{n+1}|, x_p \in I_i. \tag{12}$$

The displacement is updated using

$$F_p^{n+1} = F_p^n + \frac{\partial v^{n+1}}{\partial x}(x_p) F_p^n dt, x_p \in I_i. \tag{13}$$

While stress is updated using the appropriate constitutive model and Young's Modulus, E,

$$\sigma_p^{n+1} = \sigma_p^n + dtE \frac{\partial v^{n+1}}{\partial x}(x_p), x_p \in I_i. \tag{14}$$

3 Stability of Time Integration Using the Spigler and Vianello Approach

Spigler and Vianello [23] consider ordinary and partial differential equations of the form

$$\dot{u} = f(t,u,u), 0 < t \leq T, u(0) = u_0 \tag{15}$$

and apply the semi-implicit Euler method used by MPM to this as given by:

$$u^{n+1} = u^n + dt\ f(t_n, u^{n+1}, u^n). \tag{16}$$

It is assumed that the exact solution $\bar{u}$ to the PDE satisfies the perturbed equations given by

$$\bar{u}^{n+1} = \bar{u}^n + dt\ f(t_n, \bar{u}^{n+1}, \bar{u}^n) + \delta^{n+1}, \tag{17}$$

where δ^{n+1} is the local truncation error. Spigler and Vianello introduce a perturbed scheme given by

$$\bar{v}^{n+1} = \tilde{u}^n + dt\ f(t_{n+1}, \bar{v}^{n+1}, \tilde{u}^n) + \delta^{n+1}, \tag{18}$$

$$\tilde{u}^{n+1} = \bar{v}^{n+1} + \tilde{\sigma}^{n+1} \tag{19}$$

where $\tilde{\sigma}^{n+1}$ is a local error on the current time step. Subtracting equation (17) from (18) and adding and subtracting a term then gives

$$\bar{v}^{n+1} - u^{n+1} = \bar{u}^n - u^n + dt\ f(t_{n+1}, \bar{v}^{n+1}, \tilde{u}^n) - dt\ f(t_{n+1}, \bar{v}^{n+1}, u^n) \tag{20}$$

$$+ dt\ f(t_{n+1}, \bar{v}^{n+1}, u^n) - dt\ f(t_{n+1}, u^{n+1}, u^n) + \delta^{n+1}. \tag{21}$$

Defining the error as

$$\varepsilon^n = \bar{v}^n - u^n. \tag{22}$$

taking the inner product of equation (21) with ε^n ,using Cauchy-Schwartz on the right hand side of this equation, and taking norms and using a Lipshitz condition gives the error inequality [23]

$$||\varepsilon^{n+1}|| \leq (1 + dtK_2)||\tilde{u}^n - u^n|| + dtK_1||\varepsilon^{n+1}|| + ||\delta^{n+1}||. \tag{23}$$

While the quantity K_1 is defined by [23] via a one-sided Lipshitz condition constant, here the stronger, but equivalent, condition [13] is used

$$||f(t_n,\bar{v}^{n+1},u^n)-f(t_n,u^{n+1},u^n)|| \leq K_3||\bar{v}^{n+1}-u^{n+1}|| \tag{24}$$

that ensures that the one-sided condition also holds if K_1 is replaced by K_3. K_2 is defined by [23] as being a Lipshitz constant that satisfies the equation

$$||f(t_n,\bar{v}^{n+1},u^n)-f(t_n,\bar{v}^{n+1},\tilde{u}^n)|| \leq K_2||\tilde{u}^n-u^n||. \tag{25}$$

Regardless of which approach is used we arrive at the equation (20) in [23]:

$$||\tilde{u}^{n+1}-u^{n+1}|| \leq \frac{1+dtK_2}{(1-dtK_3)}||\tilde{u}^n-u^n|| + \frac{||\delta^{n+1}||}{(1-dtK_3)} + ||\tilde{\sigma}^{n+1}||. \tag{26}$$

The stability condition stated by [23] is then given by

$$dt(K_2+K_3) \leq 1. \tag{27}$$

In showing how to apply such stability results to non-linear problems Fekete and Farago [9,10] reference extensive earlier work, such as that of Trenogin [28] and Sanz-Serna and colleagues [21,22] which in turn references and considers the approaches of Keller and Stetter [25,15]. that uses locally Lipshitz continuous functions, In this case it is necessary to find a constant R such that a function, say, $f(x)$ satisfies a Lipshitz condition on an open ball of center z and radius L denoted by B_R which may depend on the time step see [21,22], where

$$B_L(z) := \{y \in \mathbb{R}^m : ||y-z|| \leq L\} \tag{28}$$

and the Lipshitz condition is then given on this ball by

$$||f(x)-f(y)|| \leq K||x-y||, \forall x,y \in B_L. \tag{29}$$

Furthermore the theory of Trenogin [9,10] also allows a form of stability in which the Lipshitz constant may grow in time.

In order to use the [23] theory, we now define vector quantities over the number of particles. Let the total number of particles be npt. Then vectors of particle velocities $\mathbf{v}_p^n$, and nodal velocities $\mathbf{v}_N^n$ are defined as:

$$\mathbf{v}_p^n = \left[v_1^n,...,v_{npt}^n\right]^T, \tag{30}$$

$$\mathbf{v}_N^n = \left[v_1^n,...,v_N^n\right]^T. \tag{31}$$

The vectors of particle positions $\mathbf{x}_p^n$, stresses $\boldsymbol{\sigma}_p^n$ and deformation gradients $\mathbf{f}_p^n$ are given by

$$\mathbf{x}_p^n = \left[x_1^n,...,x_{npt}^n\right]^T, \tag{32}$$

$$\boldsymbol{\sigma}_p^n = \left[\boldsymbol{\sigma}_1^n,...,\boldsymbol{\sigma}_{npt}^n\right]^T, \tag{33}$$

$$\mathbf{f}_p^n = \left[F_1^n,...,F_{npt}^n\right]^T. \tag{34}$$

The MPM vectors that correspond to those used by [23] are now defined by:

$$u^n = \begin{bmatrix} \mathbf{v}_N^n \\ \mathbf{v}_p^n \\ \sigma_p^n \\ \mathbf{f}_p^n \\ \mathbf{x}_p^n \end{bmatrix}, \text{ and } \tilde{u}^n = \begin{bmatrix} \tilde{\mathbf{v}}_N^n \\ \tilde{\mathbf{v}}_p^n \\ \tilde{\sigma}_p^n \\ \tilde{\mathbf{f}}_p^n \\ \tilde{\mathbf{x}}_p^n \end{bmatrix}. \tag{35}$$

The vector norm used is given by the 2 norm given by

$$||\mathbf{y}_p^n||_2 = \sqrt{\sum_{i=1}^{N_{tot}} (y_i^n)^2}, \text{ where } N_{tot} = N + 4Nm. \tag{36}$$

It is useful to have the elementary result

$$\left[\sum_{j=1}^{m} b_i\right]^2 \leq m \sum_{j=1}^{m} b_i^2, for\ b_i \geq 0. \tag{37}$$

As an example that helps explain results used below, the vector norm of the gradient of the particles velocity is bounded by the norm of the velocity values at nodes.

$$\left\| \frac{\partial v^{n+1}}{\partial x} \right\| = \frac{1}{h} \left[\sum_{p=1}^{npt} \left(\sum_{j=i-1}^{i+2} \gamma_{j,p} v_j^{n+1}, \right)^2 \right]^{1/2} \tag{38}$$

As there are m particles per intervals and using equation (12) and transforming the sum into one over intervals gives:

$$\left| |\frac{\partial v^{n+1}}{\partial x}| \right| \leq \frac{1}{h} \left[\sum_{i=1}^{N} m \left(\sum_{j=i-1}^{i+2} |v_j^{n+1}|, \right)^2 \right]^{1/2} \tag{39}$$

$$\leq \frac{\sqrt{m}}{h} \left[\sum_{i=1}^{N} 16 (v_i^{n+1})^2 \right]^{1/2} \tag{40}$$

$$\leq \frac{4\sqrt{m}}{h} ||v_i^{n+1}|| \tag{41}$$

4 MPM with Symplectic Euler A Integration (Stress Last)

The approach of [23] is now applied to the stress-last case as described by Bardenhagen [1] which uses the Euler-A symplectic scheme discussed by [16]. The vector form of the equations for the update of velocities, stresses and deformation gradients and then positions are given by the following equations. The vector forms of equations (7, 8) and (9) are:

$$\mathbf{v}_N^{n+1} = \mathbf{v}_N^n + dt \mathbf{H_N}(\mathbf{x}_p^n, \sigma_p^n, \mathbf{f}_p^n), \tag{42}$$

$$\mathbf{v}_p^{n+1} = \mathbf{v}_p^n + dt \mathbf{H_p}(\mathbf{x}_p^n, \sigma_p^n, \mathbf{f}_p^n). \tag{43}$$

The vector form of equations (14), (13) and (10) are written as:

$$\sigma_p^{n+1} = \sigma_p^n + dt\mathbf{S}(\mathbf{v}_N^{n+1}), \tag{44}$$

$$\mathbf{f}_p^{n+1} = \mathbf{f}_p^n + dt\mathbf{G}(\mathbf{f}_p^n, \mathbf{v}_N^{n+1}), \tag{45}$$

$$\mathbf{x}_p^{n+1} = \mathbf{x}_p^n + dt\mathbf{v}_p^{n+1}. \tag{46}$$

Using this notation and that used to define the vectors (35) the MPM method may be written as

$$\begin{bmatrix} \bar{\mathbf{v}}_N^{n+1} \\ \bar{\mathbf{v}}_p^{n+1} \\ \bar{\sigma}_p^{n+1} \\ \bar{\mathbf{f}}_p^{n+1} \\ \bar{\mathbf{x}}_p^{n+1} \end{bmatrix} - \begin{bmatrix} \mathbf{v}_N^{n+1} \\ \mathbf{v}_p^{n+1} \\ \sigma_p^{n+1} \\ \mathbf{f}_p^{n+1} \\ \mathbf{x}_p^{n+1} \end{bmatrix} = \begin{bmatrix} \bar{\mathbf{v}}_N^{p+1} \\ \bar{\mathbf{v}}_p^{n} \\ \bar{\sigma}_p^{n} \\ \bar{\mathbf{f}}_p^{n} \\ \bar{\mathbf{x}}_p^{n} \end{bmatrix} - \begin{bmatrix} \mathbf{v}_N^{n+1} \\ \mathbf{v}_p^{n+1} \\ \sigma_p^{n} \\ \mathbf{f}_p^{n} \\ \mathbf{x}_p^{n} \end{bmatrix} + dt \begin{bmatrix} \mathbf{H}_N(\tilde{\mathbf{x}}_p^n, \tilde{\sigma}_p^n, \tilde{\mathbf{f}}_p^n) - \mathbf{H}_N(\mathbf{x}_p^n, \sigma_p^n, \mathbf{f}_p^n) \\ \mathbf{H}_p(\tilde{\mathbf{x}}_p^n, \tilde{\sigma}_p^n, \tilde{\mathbf{f}}_p^n) - \mathbf{H}_p(\mathbf{x}_p^n, \sigma_p^n, \mathbf{f}_p^n) \\ \mathbf{0} \\ \mathbf{G}(\tilde{\mathbf{f}}_p^n, \mathbf{v}_N^{n+1}) - \mathbf{G}(\mathbf{f}_p^n, \mathbf{v}_N^{n+1}) \\ \mathbf{0} \end{bmatrix}$$

$$+dt \begin{bmatrix} \mathbf{0} \\ \mathbf{0} \\ \mathbf{S}(\bar{\mathbf{v}}_N^{n+1}) - \mathbf{S}(\mathbf{v}_N^{n+1}) \\ \mathbf{G}(\mathbf{f}_p^n, \bar{\mathbf{v}}_N^{n+1}) - \mathbf{G}(\mathbf{f}_p^n, \mathbf{v}_N^{n+1}) \\ \bar{\mathbf{v}}_p^{n+1} - \mathbf{v}_p^{n+1} \end{bmatrix}. \tag{47}$$

4.1 Lipshitz constants

The results of [23] require the determination of the Lipshitz constants K_2 and K_3 where:

$$\left\| \begin{bmatrix} \mathbf{H}_N(\tilde{\mathbf{x}}_p^n, \tilde{\sigma}_p^n, \tilde{\mathbf{f}}_p^n) - \mathbf{H}_N(\mathbf{x}_p^n, \sigma_p^n, \mathbf{f}_p^n) \\ \mathbf{H}_p(\tilde{\mathbf{x}}_p^n, \tilde{\sigma}_p^n, \tilde{\mathbf{f}}_p^n) - \mathbf{H}_p(\mathbf{x}_p^n, \sigma_p^n, \mathbf{f}_p^n) \\ \mathbf{0} \\ \mathbf{G}(\tilde{\mathbf{f}}_p^n, \mathbf{v}_N^{n+1}) - \mathbf{G}(\mathbf{f}_p^n, \mathbf{v}_N^{n+1}) \\ \mathbf{0} \end{bmatrix} \right\| \leq K_2 \left\| \begin{bmatrix} \bar{\mathbf{v}}_N^n - \mathbf{v}_N^n \\ \bar{\mathbf{v}}_p^n - \mathbf{v}_p^n \\ \bar{\sigma}_p^n - \sigma_p^n \\ \bar{\mathbf{f}}_p^n - \mathbf{f}_p^n \\ \bar{\mathbf{x}}_p^n - \mathbf{x}_p^n \end{bmatrix} \right\| \tag{48}$$

$$\left\| \begin{bmatrix} \mathbf{0} \\ \mathbf{0} \\ \mathbf{S}(\bar{\mathbf{v}}_N^{n+1}) - \mathbf{S}(\mathbf{v}_N^{n+1}) \\ \mathbf{G}(\mathbf{f}_p^n, \bar{\mathbf{v}}_N^{n+1}) - \mathbf{G}(\mathbf{f}_p^n, \mathbf{v}_N^{n+1}) \\ \bar{\mathbf{v}}_p^{n+1} - \mathbf{v}_p^{n+1} \end{bmatrix} \right\| \leq K_3 \left\| \begin{bmatrix} \bar{\mathbf{v}}_N^{n+1} - \mathbf{v}_N^{n+1} \\ \bar{\mathbf{v}}_p^{n+1} - \mathbf{v}_p^{n+1} \\ \bar{\sigma}_p^{n+1} - \sigma_p^{n+1} \\ \bar{\mathbf{f}}_p^{n+1} - \mathbf{f}_p^{n+1} \\ \bar{\mathbf{x}}_p^{n+1} - \mathbf{x}_p^{n+1} \end{bmatrix} \right\|. \tag{49}$$

4.2 Bounding the Lipshitz Conditions K_2

At particle position $x_p \in I_i$, the local part of the equation for K_2 is

$$\left[\mathbf{G}(\mathbf{f}_p^n, \bar{\mathbf{v}}_N^{n+1}) - \mathbf{G}(\mathbf{f}_p^n, \mathbf{v}_N^{n+1})\right]_p = F_p \frac{1}{h} \sum_{j=i-1}^{i+2} \gamma_{j,p} \Delta v_j^{n+1}, x_p \in I_i \tag{50}$$

where $\Delta v_i = \left[\bar{\mathbf{v}}_N^{n+1} - \mathbf{v}_N^{n+1}\right]_i$. Writing this as a vector equation and taking norms and using equation (41)gives:

$$||\mathbf{G}(\mathbf{f}_p^n, \bar{\mathbf{v}}_N^{n+1}) - \mathbf{G}(\mathbf{f}_p^n, \mathbf{v}_N^{n+1})|| = (\sum_{p=1}^{npt} \left(F_p \frac{1}{h} \sum_{j=i-1}^{i+2} \gamma_{j,p} \Delta v_j^{n+1} \right)^2)^{1/2},$$

$$||\mathbf{G}(\mathbf{f}_p^n, \bar{\mathbf{v}}_N^{n+1}) - \mathbf{G}(\mathbf{f}_p^n, \mathbf{v}_N^{n+1})|| \leq \frac{F_{maxp}}{h} \sqrt{m} \sum_{i=1}^{N} (\sum_{j=i-1}^{i+2} |\Delta v_j^{n+1}|)^2)^{1/2},$$

$$\leq \frac{F_{maxp}}{h} 4\sqrt{m} ||\Delta \mathbf{v}||, \qquad (51)$$

where $F_{maxp} = max_p |F_p|$. Similarly at the same particle position

$$\left[\mathbf{S}(\bar{\mathbf{v}}_N^{n+1}) - \mathbf{S}(\mathbf{v}_N^{n+1})\right]_p = E \left(\frac{1}{h} \sum_{j=i-1}^{i+2} \gamma_{j,p} \Delta v_j^{n+1} \right) \qquad (52)$$

and so using the same arguments as above

$$||\mathbf{S}(\bar{\mathbf{v}}_N^{n+1}) - \mathbf{S}(\mathbf{v}_N^{n+1})|| \leq E \frac{4\sqrt{m}}{h} ||\Delta \mathbf{v}||. \qquad (53)$$

The final equation of (49) is satisfies by a Lipshitz constant with value one. Combining these results, after noting that they apply to different parts of the right side of (49), gives

$$K_3 \leq max(1, \frac{4\sqrt{m}}{h}(E + F_{maxp})). \qquad (54)$$

4.3 Defining the Lipshitz Conditions for the Function $G(...)$ in Equation (48)

From equation (50) at particle position $x_p \in I_i$

$$\left[\mathbf{G}(\bar{\mathbf{f}}_p^n, \mathbf{v}_N^{n+1}) - \mathbf{G}(\mathbf{f}_p^n, \mathbf{v}_N^{n+1})\right]_p = (\bar{F}_p^n - F_p^n) \frac{1}{h} \sum_{j=i-1}^{i+2} \gamma_{j,p} \Delta v_j^{n+1}. \qquad (55)$$

Squaring both sides gives

$$|\left[\mathbf{G}(\bar{\mathbf{f}}_p^n, \mathbf{v}_N^{n+1}) - \mathbf{G}(\mathbf{f}_p^n, \mathbf{v}_N^{n+1})\right]_p|^2 \leq |(\bar{F}_p^n - F_p^n)^2 (\frac{1}{h} \sum_{j=i-1}^{i+2} \gamma_{j,p} \Delta v_j^{n+1})^2, p = 1, ...Nm, \qquad (56)$$

where i is defined by which $x_p \in I_i$. Summing over the number of particles p and using a similar argument as in Section 4.2 gives

$$||\left[\mathbf{G}(\bar{\mathbf{f}}_p^n, \mathbf{v}_N^{n+1}) - \mathbf{G}(\mathbf{f}_p^n, \mathbf{v}_N^{n+1})\right]|| \leq K_2^* ||(\bar{\mathbf{f}}_p -, \mathbf{f}_p)|| \qquad (57)$$

where again using equations (41) gives

$$K_2^* \leq = \frac{4}{h} \sqrt{m} ||\Delta v_j^{n+1}||. \qquad (58)$$

Hence from equations (58,54)

$$K_2^* + K_3 \leq \frac{4}{h} \sqrt{m} (E + F_{maxp} + ||\Delta v_j^{n+1}||||). \qquad (59)$$

4.4 Defining the Lipshitz Conditions for the Function $H_N(...)$ in Equation (48)

Applying the triangle inequality to the first equation in (48) gives:

$$||\mathbf{H_N}(\tilde{\mathbf{x}}_p^n,\tilde{\sigma}_p^n,\tilde{\mathbf{f}}_p^n)-\mathbf{H_N}(\mathbf{x}_p^n,\sigma_p^n,\mathbf{f}_p^n)||\leq||\mathbf{H_N}(\tilde{\mathbf{x}}_p^n,\sigma_p^n,\mathbf{f}_p^n)-\mathbf{H_N}(\mathbf{x}_p^n,\sigma_p^n,\mathbf{f}_p^n)||+$$
$$||\mathbf{H_N}(\tilde{\mathbf{x}}_p^n,\tilde{\sigma}_p^n,\mathbf{f}_p^n)-\mathbf{H_N}(\tilde{\mathbf{x}}_p^n,\sigma_p^n,\mathbf{f}_p^n)||+||\mathbf{H_N}(\tilde{\mathbf{x}}_p^n,\tilde{\sigma}_p^n,\tilde{\mathbf{f}}_p^n)-\mathbf{H_N}(\tilde{\mathbf{x}}_p^n,\tilde{\sigma}_p^n,\mathbf{f}_p^n)||. \quad (60)$$

This condition may be broken down into three parts

$$||\mathbf{H_N}(\tilde{\mathbf{x}}_p^n,\sigma_p^n,\mathbf{f}_p^n)-\mathbf{H_N}(\mathbf{x}_p^n,\sigma_p^n,\mathbf{f}_p^n)||+\leq K_{2,2}^N||\tilde{\mathbf{x}}_p^n-\mathbf{x}_p^n||, \quad (61)$$

$$||\mathbf{H_N}(\tilde{\mathbf{x}}_p^n,\tilde{\sigma}_p^n,\mathbf{f}_p^n)-\mathbf{H_N}(\tilde{\mathbf{x}}_p^n,\sigma_p^n,\mathbf{f}_p^n)||\leq K_{2,0}^N||\tilde{\sigma}_p^n-\sigma_p^n||, \quad (62)$$

$$||\mathbf{H_N}(\tilde{\mathbf{x}}_p^n,\tilde{\sigma}_p^n,\tilde{\mathbf{f}}_p^n)-\mathbf{H_N}(\tilde{\mathbf{x}}_p^n,\tilde{\sigma}_p^n,\mathbf{f}_p^n)||\leq K_{2,1}^N||\tilde{\mathbf{f}}_p^n-\mathbf{f}_p^n||. \quad (63)$$

For which, by using the properties of vector norms, it follows that

$$K_2\leq K_{2,0}^N+K_{2,1}^N+K_{2,2}^N. \quad (64)$$

The ith component of the left side of equation (62) may be written as

$$\left[\mathbf{H}_N(\tilde{\mathbf{x}}_p^n,\tilde{\sigma}_p^n,\mathbf{f}_p^n)-\mathbf{H}_N(\tilde{\mathbf{x}}_p^n,\sigma_p^n,\mathbf{f}_p^n)\right]_i=\tilde{a}_i^{n+1} \quad (65)$$

where

$$\tilde{a}_i^{n+1}=\frac{1}{m}\sum_{x_p\in I_{i+1}\cup I_i\cup I_{i-1}\cup I_{i-2}}D_{ip}^{n*}\delta\sigma_p^n|F_p^n|. \quad (66)$$

and

$$\delta\sigma_p^n=\tilde{\sigma}_p^n-\sigma_p^n. \quad (67)$$

Upon defining

$$DF^n=max_p|D_{ip}^{n*}F_p^n| \quad (68)$$

and noting that $|D_{ip}^{n*}|\leq 1$ allows equation (65) to be written as

$$|\left[\mathbf{H}_N(\tilde{\mathbf{x}}_p^n,\tilde{\sigma}_p^n,\mathbf{f}_p^n)-\mathbf{H}_N(\tilde{\mathbf{x}}_p^n,\sigma_p^n,\mathbf{f}_p^n)\right]_i|\leq\frac{1}{m}F_{maxp}|\sum_{x_p\in I_{i+1}\cup I_i\cup I_{i-1}\cup I_{i-2}}\delta\sigma_p^n|. \quad (69)$$

Squaring both sides, summing over i nodes and using (37) gives

$$||\mathbf{H}_N(\tilde{\mathbf{x}}_p^n,\tilde{\sigma}_p^n,\mathbf{f}_p^n)-\mathbf{H}_N(\tilde{\mathbf{x}}_p^n,\sigma_p^n,\mathbf{f}_p^n)||^2\leq(\frac{1}{m}F_{maxp})^2 4m\sum_{x_p\in I_{i+1}\cup I_i\cup I_{i-1}\cup I_{i-2}}(\delta\sigma_p^n)^2 \quad (70)$$

which after taking the square root gives and using equation (41) gives

$$||\mathbf{H}_N(\tilde{\mathbf{x}}_p^n,\tilde{\sigma}_p^n,\mathbf{f}_p^n)-\mathbf{H}_N(\tilde{\mathbf{x}}_p^n,\sigma_p^n,\mathbf{f}_p^n)||\leq(\frac{1}{m}F_{maxp})4\sqrt{m}||\delta\sigma|| \quad (71)$$

and so

$$K_{2,0}^N\leq\frac{4}{\sqrt{m}}F_{maxp}. \quad (72)$$

For equation (63) the pth component of the vector $\delta\mathbf{f}$ is defined by

$$\delta f_p^n = \tilde{f}_p^n - f_p^n. \tag{73}$$

After defining

$$\sigma_{maxp} = max_p|\sigma_p^n|, \tag{74}$$

and a similar argument as above in equations 69) to 72) leads to

$$|\left[\mathbf{H}_N(\tilde{\mathbf{x}}_p^n, \tilde{\sigma}_p^n, \tilde{\mathbf{f}}_p^n) - \mathbf{H}_N(\tilde{\mathbf{x}}_p^n, \tilde{\sigma}_p^n, \mathbf{f}_p^n)\right]_i| \leq \frac{1}{m}\sigma_{maxp} \sum_{x_p \in I_{i+1}\cup I_i \cup I_{i-1}\cup I_{i-2}} |\delta F_p^n|. \tag{75}$$

A similar argument as in equations (70, 71,72) then gives

$$K_{2,1}^N \leq \frac{4}{\sqrt{m}}\sigma_{maxp}. \tag{76}$$

In the case of equation (61) Berzins [6] shows that the original MPM method does not satisfy a Lipshitz condition. In contrast for the GIMP method, see (29) and Figure 4b in [24], it follows that

$$|D_{ip}^{n*}(\tilde{x}_p^n) - D_{ip}^{n*}(x_p^n)| \leq \frac{2}{l}|\tilde{x}_p^n - x_p^n| \tag{77}$$

where l is the nominal width associated with the particle. Let

$$\sigma F^n = max_p|F_p^n\sigma_p^n|, \tag{78}$$

then the change in acceleration in the left side of equation (61) as denoted by δa_i^{n+1} is given by

$$\delta a_i^{n+1} = \frac{1}{m} \sum_{x_p \in I_{i+1}\cup I_i \cup I_{i-1}\cup I_{i-2}} \delta D_{jp}^{n*}\sigma_p^n|F_p^n|, where\ x_p \in I_j. \tag{79}$$

and satisfies the inequality

$$(\delta a_i^{n+1})^2 \leq \left(\frac{2}{lm}\sigma F^n\right)^2 \left(\sum_{p\in I_{i+1}\cup I_i\cup I_{i-1}\cup I_{i-2}} |\delta x_p^n|\right)^2 \tag{80}$$

where

$$\delta x_p^n = \tilde{x}_p^n - x_p^n. \tag{81}$$

It then follows that

$$(\delta a_i^{n+1})^2 \leq \left(\frac{2}{lm}\sigma F^n\right)^2 4m \sum_{p\in I_{i+1}\cup I_i\cup I_{i-1}\cup I_{i-2}} (\delta x_p^n)^2 \tag{82}$$

and after summing over p and taking square roots that

$$||\delta a_i^{n+1}|| \leq \left(\frac{2}{lm}\sigma F^n\right) 4\sqrt{m}||\delta x_p^n|| \tag{83}$$

Similar arguments as in the previous section give the result

$$K_{2,2}^N \leq \frac{8}{\sqrt{ml}}\sigma F^n. \tag{84}$$

4.5 Defining the Lipshitz Conditions for the Function $H_p(...)$ in Equation (48)

Again this equation can be broken down into three parts

$$||\mathbf{H}_p(\tilde{\mathbf{x}}_p^n,\tilde{\sigma}_p^n,\tilde{\mathbf{f}}_p^n)-\mathbf{H}_p(\mathbf{x}_p^n,\sigma_p^n,\mathbf{f}_p^n)|| \le ||\mathbf{H}_p(\tilde{\mathbf{x}}_p^n,\sigma_p^n,\mathbf{f}_p^n)-\mathbf{H_p}(\mathbf{x}_p^n,\sigma_p^n,\mathbf{f}_p^n)||+$$
$$||\mathbf{H}_p(\tilde{\mathbf{x}}_p^n,\tilde{\sigma}_p^n,\mathbf{f}_p^n)-\mathbf{H}_p(\tilde{\mathbf{x}}_p^n,\sigma_p^n,\mathbf{f}_p^n)|| + ||\mathbf{H}_p(\tilde{\mathbf{x}}_p^n,\tilde{\sigma}_p^n,\tilde{\mathbf{f}}_p^n)-\mathbf{H}_p(\tilde{\mathbf{x}}_p^n,\tilde{\sigma}_p^n,\mathbf{f}_p^n)|| \quad (85)$$

and three Lipshitz constants used to bound the terms on the right side of this equation:

$$||\mathbf{H}_p(\tilde{\mathbf{x}}_p^n,\sigma_p^n,\mathbf{f}_p^n)-\mathbf{H}_p(\mathbf{x}_p^n,\sigma_p^n,\mathbf{f}_p^n)|| \le K_{2,2}^p||\tilde{\mathbf{x}}_p^n-\mathbf{x}_p^n|| \quad (86)$$

$$||\mathbf{H}_p(\tilde{\mathbf{x}}_p^n,\tilde{\sigma}_p^n,\mathbf{f}_p^n)-\mathbf{H}_p(\tilde{\mathbf{x}}_p^n,\sigma_p^n,\mathbf{f}_p^n)|| \le K_{2,0}^p||\tilde{\sigma}_p^n-\sigma_p^n|| \quad (87)$$

$$||\mathbf{H}_p(\tilde{\mathbf{x}}_p^n,\tilde{\sigma}_p^n,\tilde{\mathbf{f}}_p^n)-\mathbf{H}_p(\tilde{\mathbf{x}}_p^n,\tilde{\sigma}_p^n,\mathbf{f}_p^n)|| \le K_{2,1}^p||\tilde{\mathbf{f}}_p^n-\mathbf{f}_p^n|| \quad (88)$$

Equation (87) is considered first using the definition in (67). Let

$$\tilde{a}_i^{n+1} = \frac{1}{m}\sum_{p\in I_{i+1}\cup I_i\cup I_{i-1}\cup I_{i-2}} D_{jp}^{n*}\delta\sigma_p^n|F_p^n|,\ for\ x_p\in I_j \quad (89)$$

$$\tilde{a}_{i+1}^{n+1} = \frac{1}{m}\sum_{p\in I_{i+2}\cup I_{i+1}\cup I_i\cup I_{i-1}} D_{jp}^{n*}\delta\sigma_p^n|F_p^n|,\ for\ x_p\in I_j \quad (90)$$

and note that from equations (7,9) the pth component of equation (87) is

$$\left[\mathbf{H}_p(\tilde{\mathbf{x}}_p^n,\tilde{\sigma}_p^n,\mathbf{f}_p^n)-\mathbf{H}_p(\tilde{\mathbf{x}}_p^n,\sigma_p^n,\mathbf{f}_p^n)\right]_p =$$
$$\left[\lambda_{i+1,p}\tilde{a}_{i+1}^{n+1}+\lambda_{i,p}\tilde{a}_i^{n+1}+\lambda_{i-1,p}\tilde{a}_{i-1}^{n+1}+\lambda_{i-2,p}\tilde{a}_{i-2}^{n+1}\right]. \quad (91)$$

Using the same approach as in equations (69) to (71) gives the inequality

$$|\left[\mathbf{H}_p(\tilde{\mathbf{x}}_p^n,\tilde{\sigma}_p^n,\mathbf{f}_p^n)-\mathbf{H}_p(\tilde{\mathbf{x}}_p^n,\sigma_p^n,\mathbf{f}_p^n)\right]_p| \le= \frac{F_{maxp}}{m}\sum_{x_p\in I_{i+2}\cup I_{i+1}\cup I_i\cup I_{i-1}\cup I_{i-2}}|\delta\sigma_p^n| \quad (92)$$

and, as above, summing over 5 intervals and 5m particles and using (41) gives

$$K_{2,0}^p \le \frac{5}{\sqrt{m}}\,F_{maxp} \quad (93)$$

For equation (88) a similar argument as above again leads to

$$|\left[\mathbf{H}_p(\tilde{\mathbf{x}}_p^n,\tilde{\sigma}_p^n,\tilde{\mathbf{f}}_p^n)-\mathbf{H}_p(\tilde{\mathbf{x}}_p^n,\tilde{\sigma}_p^n,\mathbf{f}_p^n)\right]_i| \le \frac{1}{m}\sigma_{maxp}\sum_{x_p\in I_{i-2}\cup I_{i-1}\cup I_i\cup I_{I+1}\cup I+2}|\delta F_p^n| \quad (94)$$

and then

$$K_{2,1}^p \le \frac{5}{\sqrt{m}}\sigma_{maxp}. \quad (95)$$

The final case gives

$$|\left[\mathbf{H}_p(\tilde{\mathbf{x}}_p^n,\sigma_p^n,\mathbf{f}_p^n)-\mathbf{H}_p(\mathbf{x}_p^n,\sigma_p^n,\mathbf{f}_p^n)\right]_p| \le \frac{2}{lm}\sigma F^n\sum_{x_p\in I_{i-2}\cup I_{i-1}\cup I_i\cup I_{i+1}\cup I_{i+2}}|\delta x_p^n| \quad (96)$$

resulting in

$$K_{2,2}^p \le \frac{10}{\sqrt{ml}}\,\sigma F^n. \quad (97)$$

4.6 Stability Condition

It is now possible to define the constants in the stability condition (27). The constant K_3 is defined by equation (58). Collecting together the different local Lipshitz conditions with respect to the vectors multiplied by those constants from equations (61,62,63,86,87,88) gives

$$K_2 \leq K_{2,0}^N + K_{2,0}^P + K_{2,1}^N + K_{2,1}^P + K_2^* + K_{2,2}^N + K_{2,2}^P \tag{98}$$

Bringing together (72,76,84,93,95,97), then gives

$$K_2 \leq K_2^* + \frac{9}{\sqrt{m}}(F_{maxp} + \sigma_{maxp} + \frac{2}{l}\sigma F_n). \tag{99}$$

The only part of this that is similar to a conventional CFL type condition is the coefficient K_2^*, however even this term depends on the velocity gradients. This expression gives additional weight to the comments in [19] about how more than a conventional CFL condition is needed. Combining equations (98) and (99) in (27) gives the stability condition

$$dt \leq 1/(K_3 + K_2^* + \frac{9}{\sqrt{m}}(F_{maxp} + \sigma_{maxp} + \frac{2}{l}\sigma F_n)) \tag{100}$$

Combining results from equations (59) and (100) and using the bound on D coefficients from equation (68) we get

$$dt \leq \frac{h\sqrt{m}}{4m(E + F_{maxp} + ||v_i||) + 9h(F_{maxp} + \sigma_{maxp} + \frac{2}{l\sqrt{m}}\sigma F_n)} \tag{101}$$

This result reflects the form of the original equations in that the Young's modulus constant E appears in its original form in the equation (14) for the evolution of stress. In contrast the speed of sound heuristic used by codes such as [12] gives rise to the equation:

$$dt_{sound} \leq h/\sqrt{E} \tag{102}$$

This difference between e and $\sqrt{E}$ occurs in part by noting that when the standard wave equation $U_{tt} = c^2 U_x x$ is written as a pair of first order equations.

$$\frac{\partial U}{\partial t} = c\frac{\partial W}{\partial x} \tag{103}$$

$$\frac{\partial W}{\partial t} = c\frac{\partial U}{\partial x} \tag{104}$$

where c is the sound speed. The same approach can be used here by defining

$$\hat{\sigma} = \frac{\sigma}{\sqrt{E}} \tag{105}$$

This means that the equation for the evolution of stress (14) may be rewritten as:

$$\frac{\partial \hat{\sigma}}{\partial t} = \sqrt{E}\frac{\partial v}{\partial x} \tag{106}$$

Hence the associated Lipshitz constant K_3 involves $\sqrt{E}$ instead of E. and the acceleration equation (7) may be rewritten as

$$a_i^{n+1} = \frac{-\sqrt{E}}{m}\Big(\sum_{x_p\in I_{i-2}} D_{ip}^{n*}\hat{\sigma}_p^n|F_p^n| + \sum_{x_p\in I_{i-1}} D_{ip}^{n*}\hat{\sigma}_p^n|F_p^n| + \sum_{x_p\in I_i} D_{ip}^{n*}\hat{\sigma}_p^n|F_p^n| + \sum_{x_p\in I_{i+1}} D_{ip}^{n*}\hat{\sigma}_p^n|F_p^n|\Big) \tag{107}$$

and the associated Lipshitz constants are appropriately multiplied by $\sqrt{E}$. Once this is done then this scaling filters through the analysis to give modified Lipshitz constants and in a straightforward manner arrive at the modified stability condition.

$$dt \leq \frac{h\sqrt{m}}{4m(\sqrt{E}+F_{maxp}+||v_i||)+9h\sqrt{E}(F_{maxp}+\sigma_{maxp}+\frac{2}{l\sqrt{m}}\sigma F_n)} \tag{108}$$

5 Computational Experiments

5.1 Model Problem

In order to illustrate the above results the model problem used by Gritton and Berzins [11] will be employed. This problem is defined by:

$$\sigma = P = E\frac{\partial u}{\partial X} = E(F-1), \tag{109}$$

where E is the Young's modulus. The rate of change of stress is then computed as,

$$\dot{\sigma} = E(\dot{F}), \tag{110}$$

$$= E(lF), \tag{111}$$

where l is the velocity gradient in the spatial description.

The problem considered is a 1D bar problem, following similar examples in [24]. The analytic solutions for displacement and velocity defined in the material description are:

$$u(X,t) = Asin(2\pi X)sin(c\pi t), \tag{112}$$

$$\frac{\partial u}{\partial t} = Ac\pi sin(2\pi X)cos(c\pi t), \tag{113}$$

where $c = \sqrt{E/\rho_o}$ and A is the maximum displacement. The constitutive model is defined in Equation (109) and the body force is,

$$b(X,t) = 3A(c\pi)^2 u(X,t). \tag{114}$$

The initial spatial discretization uses two evenly spaced particles per cell with the spatial domain being $[0,1]$. The periodic nature of the analytic solution means that both periodic boundary conditions and zero Dirichlet boundary conditions are both

appropriate. The initial conditions for the updated Lagrangian description of the particles are:

$$F = 1, \tag{115}$$

$$x_p = X_p^0, \tag{116}$$

$$V_p = V_p^0. \tag{117}$$

For the 1d bar problem the cell width is $h = 10^{-2}$, the material density is $\rho_0 = 1$ and the time interval is [0,1], The Young's modulus is varied across the values $E = 10^4, 10^3, 256, 64, 16, 4$, the maximum displacement is $A = 0.015$, and $A = 0.05$ and the time step values used are $dt = 10^{-5}, 10^{-4}, 10^{-3}, 10^{-2}$. In both these cases for the values given of A it should be noted that with the use of the above parameters particles will cross from one cell to another.

5.2 MPM Methods used in Experiments

Initial experiments were undertaken with both the standard MPM method using linear basis functions at the nodes and delta functions at the particles analyzed by Berzins [6] and the MPM GIMP paper [24] as describe by Steffen et al. [24]. These experiments were run with fixed time steps as shown in Table 1 in which the time step, dt is varied appropriately. A value of * indicates instability when particles leave the domain due to too large a time step being used. In all cases just running with the speed of sound caused the code to fail. The number of grid crossings varies greatly. Table 2 shows this variation. The results in Table 1 show that the derived stability bounds while obviously conservative, give numerical errors that are close to the minimum possible with the given mesh and particle distribution.

In order to illustrate some of the challenges that arise with these calculations, more detailed results are shown for the case when $E = 1.e+4$ with $A = 6.0E-2$. Figure 1 shows the values of displacement velocity and Stress at the end of integration after 100,000 steps in this case. Figure 2 shows the errors in U, the value of the stable time steps given by equation (108) and the number of grid crossings with GIMP and a time step of 1E-5. Figure 3 shows the same results with a time step of 1E-4. The top part of Figure 3 shows the rapid increase in error at about 8500 steps at which point the calculation fails. The middle sub figure shows that the projected stable step size shrinks in response to the increased values of stress and velocity at that point. There also appear to be more grid-crossing errors than if a smaller time step is used, as is shown by comparing the bottom part of figures 2 and 3.

6 Summary

This approach addresses the non-linearity of the MPM method by deriving stability bounds using the approach of Spigler and Vianello. The bounds, while clearly conservative, do provide a reasonable limit for the time step to be used. The approach used

Table 1 Accuracy and Stability

	A=1.5e-2	E = 10000			A=5e-2	E =10000	
dt	Meth	dt Stable	Max Error	dt	Meth	dt stable	Max Error
	MPM	9.0e-5	5.1e-5		MPM	*	*
1e-4	GIMP	4.8e-6	3.8e-5	1e-4	GIMP	*	*
	MPM	8.6e-5	3.6e-4		MPM	*	*
1e-5	GIMP	4.e-6	5.1e-5	1e-5	GIMP	8.7e-7	1.7e-2
	MPM	8.2e-5	6.4e-4		MPM	*	*
1e-6	GIMP	4.7e-6	5.5e-5	1e-6	GIMP	7.9e-7	1.0e-2

	A=1.5e-2	E = 1000			A=5e-2	E =1000	
dt	Meth	dt Stable	Max Error	dt	Meth	dt stable	Max Error
	MPM	4.2e-4	2.0e-4		MPM	*	*
1e-3	GIMP	3.8e-5	1.8e-4	1e-4	GIMP	8.6e-6	4.4e-3
	MPM	4.2e-4	7.9e-5		MPM	*	*
1e-4	GIMP	3.9e-5	4.5e-5	1e-5	GIMP	8.6e-3	4.2e-2
	MPM	4.2e-4	1.2e-4		MPM	*	*
1e-5	GIMP	3.9e-5	5.6e-5	1e-6	GIMP	8.8e-6	4.4e-2
	MPM	4.2e-4	7.9e-5		MPM	*	*
1e-6	GIMP	3.9e-5	5.6e-5	1e-7	GIMP	8.6e-6	4.4e-2

	A=1.5e-2	E = 256			A=5e-2	E =256	
dt	Meth	dt Stable	Max Error	dt	Meth	dt stable	Max Error
	MPM	9.1e-4	6.2e-5		MPM	*	*
1e-3	GIMP	1.2e-4	5.2e-5	2.0e-3	GIMP	4.2e-5	2.4e-3
	MPM	9.1e-4	6.7e-5		MPM	6.0e-4	9.0e-3
1e-4	GIMP	1.2e-4	2.2e-5	1e-3	GIMP	4.5e-4	2.4e-3
	MPM	9.0e-4	1.0e-4		MPM	5.9e-4	6.8e-3
1e-5	GIMP	1.2e-4	2.3e-5	1e-4	GIMP	4.1e-5	2.9e-3
	MPM	9.0e-4	8.2e-5		MPM	*	*
1e-6	GIMP	1.2e-4	2.3e-5	1e-5	GIMP	3.8e-5	2.8e-3

	A=1.5e-2	E = 64			A=5e-2	E =64	
dt	Meth	dt Stable	Max Error	dt	Meth	dt stable	Max Error
	MPM	1.8e-3	4.6e-5		MPM	1.4e-3	8.1e-3
1e-3	GIMP	3.6e-4	1.8e-5	2e-3	GIMP	1.5e-4	7.8e-4
	MPM	1.8e-3	1.8e-5		MPM	1.4e-3	1.0e-2
1e-4	GIMP	3.7e-4	6.2e-6	1e-3	GIMP	1.5e-4	5.1e-4
	MPM	1.8e-3	7.6e-5		MPM	1.4e-3	7.5e-3
1e-5	GIMP	3.7e-4	7.4e-6	1e-4	GIMP	1.5e-4	7.0e-4
	MPM	1.8e-3	8.2e-5		MPM	1.3e-3	7.8e-3
1e-6	GIMP	3.7e-4	7.5e-5	1e-5	GIMP	1.4e-4	7.2e-4

	A=1.5e-2	E = 16			A=5e-2	E =16	
dt	Meth	dt Stable	Max Error	dt	Meth	dt stable	Max Error
	MPM	3.4e-3	4.3e-5		MPM	2.9e-3	5.0e-3
1e-3	GIMP	9.6e-4	9.1e-6	2e-3	GIMP	4.6e-4	1.5e-4
	MPM	3.4e-3	5.7e-5		MPM	2.8e-3	1.0e-2
1e-4	GIMP	9.6e-4	6.0e-6	1e-3	GIMP	4.6e-4	1.0e-4
	MPM	3.4e-3	6.2e0-5		MPM	2.8e-3	6.6e-3
1e-5	GIMP	9.6e-4	6.0e-6	1e-4	GIMP	4.6e-4	1.2e-4
	MPM	3.4e-3	6.3e-5		MPM	2.7e-3	3.7e-3
1e-6	GIMP	9.6e-4	6.0e-6	1e-5	GIMP	4.6e-4	1.7e-4

	A=1.5e-2	E = 4			A=5e-2	E = 4	
dt	Meth	dt Stable	Max Error	dt	Meth	dt stable	Max Error
	MPM	5.7e-3	4.7e-5		MPM	5.0e-2	3.4e-3
1e-3	GIMP	2.2e-3	6.8e-6	1.2e-3	GIMP	1.2e-3	1.1e-3
	MPM	5.7e-3	4.7e-5		MPM	4.0e-3	2.8e-3
1e-4	GIMP	2.1e-3	6.8e-6	1e-2	GIMP	1.0e-3	7.0e-4
	MPM	5.7e-3	5.3e-5		MPM	5.0e-3	4.8e-3
1e-5	GIMP	2.1e-3	6.0e-6	1e-3	GIMP	1.2e-3	8.4e-5
	MPM	5.7e-3	5.5e-5		MPM	4.8e-3	2.7e-3
1e-6	GIMP	2.1e-3	6.0e-6	1e-4	GIMP	1.2e-3	8.4e-5

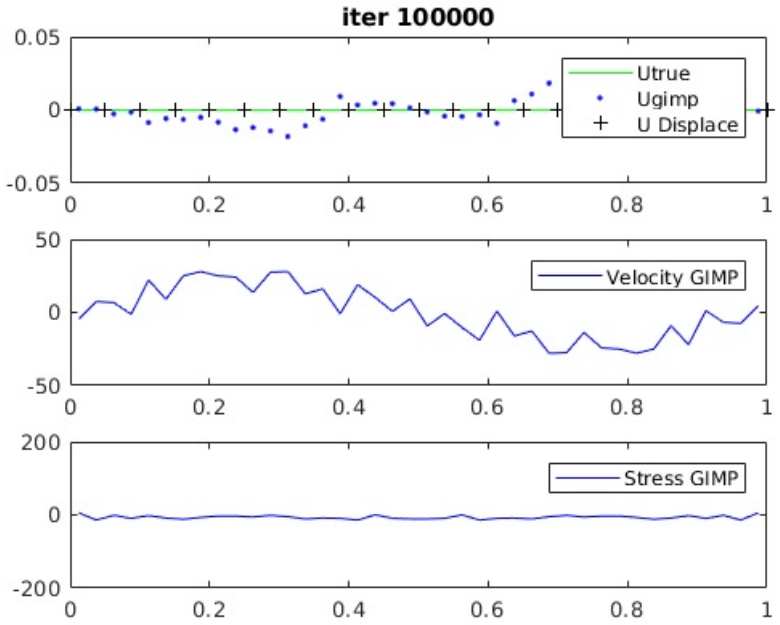

Fig. 1 1d Bar, Displacement velocity and stress for GIMP, dt=1E-5

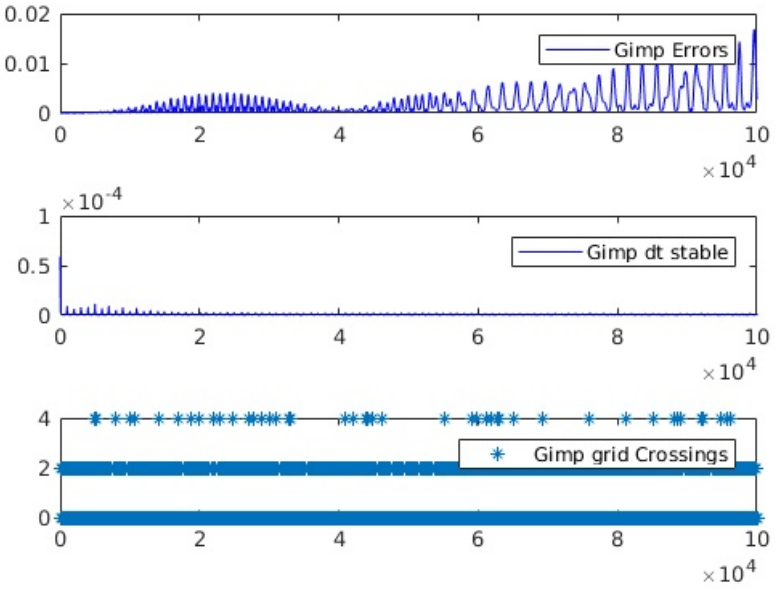

Fig. 2 1d Bar, Error vs Time steps for GIMP, dt=1E-5

Table 2 Approximate Number of Mesh Crossings For Different E values and Speed of Sound time step

E	4	16	64	256	1000	10000
A=1.5e-2	300	600	1300	2500	5000	15000
A=5.0e-2	1000	2000	4000	8000	16000	55000
dt_{sound}	0.5	0.25	0.125	0.0625	0.03132	0.01

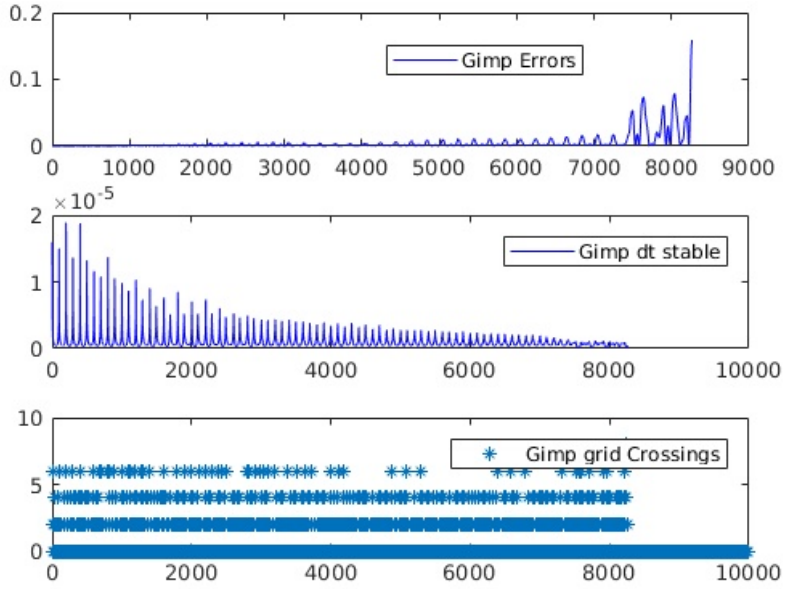

Fig. 3 1d Bar, GIMP Blowup with dt = 1E-4

here is quite general as it uses a quite general ODE form and only general information about stencils. It is thus possible to extend the idea to other variants of MPM and also to to more complex physical problems in more than one space dimension. For example in early drafts of this paper similar analysis to that above led to the same stability bounds for the stress-first version of MPM, while noting that the conservation properties of the methods are quite different [1].

As mentioned above the bounds derived here do not address the ringing instability, though by excluding the original MPM method and by limiting the time step they give rise to stable solutions for the model problem when instability does occur for larger time steps. There is a need to address this issue in future work.

Acknowledgements

Chris Gritton is thanked for the use of his code for the model problem used to obtain the results shown in Section 6. This research was partially sponsored by the Army

Research Laboratory under Cooperative Agreement Number W911NF-12-2-0023. The views and conclusions contained in this document are those of the authors and should not be interpreted as representing the official policies, either expressed or implied, of the Army Research Laboratory or the U.S. Government.

Conflict of Interest

The author states that there is no conflict of interest.

References

1. S. Bardenhagen, Energy conservation error in the material point method for solid mechanics, Journal of Computational Physics, 180, 2002, 383-403.
2. S. Bardenhagen and E. Kober, The generalized interpolation material point method, Computer Modeling in Engineering and Science, 5 (2004), 477-495.
3. T. Belytschko, Y. Guo, W. Kam Liu and S. Ping Xiao, A unified stability analysis of meshless particle methods, International Journal for Numerical Methods in Engineering, Vol. 48, no. 9, 1359–1400,2000.
4. T. Belytschko, Y. Krongauz, J. Dolbow, and C. Gerlach, *On the completeness of meshfree particle methods*, International Journal for Numerical Methods in Engineering, 43 (1998), pp. 785–819.
5. T. Belytschko and S. Xiao, *Stability analysis of particle methods with corrected derivatives*, Computers and Mathematics with Applications, 43 (2002), pp. 329 – 350.
6. M. Berzins. Non-linear Stability of MPM. Proceedings of V International Conference on Particle-based Methods Fundamentals and Applications PARTICLES 2017 P. Wriggers, M. Bischoff, E. O nate, D.R.J. Owen, & T. Zohdi (Eds)
7. J. Brackbill, The ringing instability in particle-in-cell calculations of low-speed flow, Journal of Computational Physics, 75, 1988, 469-492.
8. G. A. Dilts, Moving-least-squares-particle hydrodynamics consistency and stability, International Journal for Numerical Methods in Engineering, 44, 1999, 1115-1155.
9. I. Fekete and I. Farago, Stability concepts and their applications. Computers & Mathematics with Applications, 67,12, pp. 2158 - 2170, 2014.
10. I. Farago, M.E. Mincsovics and I. Fekete, Notes on the basic notions in non-linear numerical analysis, EJQTDE, Proc. 9th Coll. QTDE (2012), (6), pp. 122.
11. C.E. Gritton and M. Berzins, Improving Accuracy In the MPM Methods by Using a Null Spaces Filter, Comp. Part. Mech. 2017, 4 131-142.
12. C. Gritton, J. Guilkey, J. Hooper, D. Bedrov, R. M. Kirby and M. Berzins, Using the material point method to model chemical/mechanical coupling in the deformation of a silicon anode. Modelling and Simulation in Materials Science and Engineering, Vol 25, no 4, 2017
13. W. Hundsdorfer and J.G Verwer, Numerical Solution of Time Dependent Advection-Diffusion-Reaction Equations. Springer Series in Computational Mathematics 33, 2003.
14. G. R. JOHNSON AND S. R. BEISSEL, *Normalized smoothing functions for sph impact computations*, International Journal for Numerical Methods in Engineering, 39 (1996), pp. 2725–2741.
15. H.B. Keller, Approximation methods for non-linear problems with application to two-point boundary value problems, Math. Comp. 130 (1975) 464474.
16. B. Leimkuhler and S. Reich, Simulating Hamiltonian dynamics. Canbridge Monographs on Applied and Computational Science. Cambridge University Press 2004.
17. J.C. Lpez-Marcos, J.M. Sanz-Serna, A definition of stability for non-linear problems, i Numer. Treat. Differ. Equ. 104 (1988) 216226.
18. J.J. Monaghan, *SPH without a Tensile Instability*, Journal of Computational Physics, Volume 159, Issue 2, 10 April 2000, Pages 290-311,
19. M. Gong, Improving the Material Point Method, Ph.D. thesis, The University of New Mexico (2015). http://hdl.handle.net/1928/30386
20. M. Ortiz, A note on energy conservation and stability of non-linear time-stepping algorithms. Computers and Structures 24, 1, 1986, 167-168.

21. J.M. Sanz-Serna, Two topics in non-linear stability, in: i Advances in Numerical Analysis, vol. I, Oxford Sci. Publ., Oxford Univ. Press, New York, 1991, pp. 147174.
22. J.M. Sanz-Serna, C. Palencia, A general equivalence theorem in the theory of discretization methods, Math. Comp. 45 (171) (1985) 143152.
23. R. Spigler and M, Vianello, Convergence analysis of the semi-implicit Euler method for abstract evolution equations. Numer. Func. Anal. and Opt.16, 1995, 5-6, 785-803.
24. M. Steffen, P.C. Wallstedt, J.E. Guilkey, R.M. Kirby and M. Berzins, Examination and Analysis of Implementation Choices within the Material Point Method (MPM), Computer Modeling in Engineering & Sciences, 2008, 31, 2, 107-127.
25. H.J. Stetter, Analysis of Discretization Methods for Ordinary Differential Equations, i Springer, Berlin, 1973. i
26. Sulsky D, Chen Z and Schreyer HL A particle method for history-dependent materials. Comput. Meths in Appl Mech. and Engng 118 (1994):179-196.
27. Sulsky D, Zhou S-J and Schreyer HL Application of a particle-in-cell method to solid mechanics. Computer Physics Communications 87 (1995):236-252 .
28. V.A Trenogin, Functional Analysis (in Russian), Nauka, Moscow, 1980.
29. P. C. Wallstedt and J. E. Guilkey, An evaluation of explicit time integration schemes for use with the generalized interpolation material point method. J. Comput. Phys. 2008, 227, 22, 9628-9642.